

Initial Studies of Photocatalytic Discolouration of Methyl Orange by Using ZnO Nanostructures

Daniel A. R. Souza^{*}, Marivone Gusatti, Caroline Sanches, Vítor M. Moser, Nivaldo C. Kuhnén, Humberto G. Riella

Programa de Pós-Graduação em Engenharia Química, Universidade Federal de Santa Catarina, Campus Universitário, Trindade, Florianópolis, Santa Catarina, 88040-900, Brazil
daniel.arg@gmail.com

ZnO nanorods were successfully fabricated by a simple chemical reaction from zinc chloride (ZnCl_2) and sodium hydroxide (NaOH) in 3 h refluxing at 60 °C and 80 °C. The crystallinity of the grown products was analyzed by X-ray diffraction technique revealing the as prepared ZnO samples have hexagonal wurtzite structure. Their morphology was investigated by using TEM, which showed that nanorods of 25 nm (80 °C) – 30 nm (60 °C) in average diameter had been formed. The photocatalytic property of ZnO nanoparticles were investigated via methyl orange as a model organic compound under UV light irradiation.

1. Introduction

Due to their size and shape dependent properties, nano-dimensional semiconductor materials have innumerable applications. Zinc oxide (ZnO) is mostly a n-type, II–VI, wide direct band gap, semiconducting material (Huang et al., 2001) with a broad range of uses including optoelectronic devices, lasers (Johnson et al., 2001), varistors (Viswanatha et al., 2004), solar cells (Liu et al., 2007), transistors, gas sensors (Duffy et al., 2007), cosmetics (Lu et al., 2009), photocatalysts (Parida et al., 2006) and pigments (Kanade et al., 2006).

ZnO-based materials have excellent prospects for high temperature optoelectronic applications due to their high exciton binding energy of 60 MeV and high optical gain (320 cm^{-1}) at room temperature (Wahab et al., 2011). ZnO has several desirable characteristics such as high transmittance in the visible region, photocatalytic properties (Kajbafvala et al., 2012), oxidation, removal of pollutants (Caglar et al., 2009), low electrical resistivity and non-toxicity (Major et al., 2009).

There are various processes for the purification of pollutants in both water and air such as advanced oxidation that uses ZnO (Wang et al., 2005). Among the advanced oxidation processes, heterogeneous photocatalysis in the presence of sunlight/UV light as the energy source have been extensively studied (Kajbafvala et al., 2012). Photocatalytic reactions are those in which the semiconductor particle absorbs a photon with greater energy than the band gap. Subsequently, the electron is excited from the valence band to the conduction band producing the electron/hole pair and the oxidation and/or reduction of the adsorption substrates begins (Chakrabarti et al., 2008). These oxidation and reduction reactions can cause the degradation of pollutants and convert them to non-toxic compounds (Kenanakis and Katsarakis, 2010).

Several routes are employed for the synthesis of ZnO nanostructures including organometallic (Rataboul et al., 2002), vapor decomposition (Siah et al., 2000), thermal decomposition, hydrothermal (Chen et al., 2007), precipitation, sol-gel (Wang et al., 2003), synthesis by vapor phase (Haase et al., 1998), sol-gel (Hu and Chen, 2008) and solochemical (Gusatti et al., 2009).

Of these methods, the solochemical technique has several advantages over the others such as low cost, rapid synthesis and easy handling (Gusatti et al., 2011). This technique does not require vacuum conditions, surfactants, and by employing different experimental conditions, one can control the size and morphology of the ZnO nanostructures (Gusatti et al., 2012).

In this paper, the ZnO nanostructures were prepared by a simple solochemical method at different reaction temperatures. The structure, phase and morphology of synthesized products were investigated by the standard characterization techniques. In addition to these properties, the photocatalytic activity of synthesized ZnO samples were observed in presence of methyl orange and compared to commercial ZnO.

2. Experimental

2.1 Preparation of ZnO nanostructures

In this study, the ZnO samples were prepared by the solochemical method using 0.5 mol.L^{-1} zinc chloride (ZnCl_2) solution mixed with a 1.0 mol.L^{-1} sodium hydroxide (NaOH) solution. These reagents were of analytical grade and were used without further purification. All samples were produced by the same experimental procedure described in Gusatti et al. (2010). However, in this work, the materials were synthesized by chemical reactions between ZnCl_2 solutions at room temperature and heated alkaline solutions at temperatures of 60°C and 80°C . Bulk zinc oxide and methyl orange with analytical grade were purchased commercially. The photocatalytic activity of the ZnO samples was compared with that of commercial ZnO. The commercial methyl orange (dye) was used like a model organic compound.

2.2 Analysis

The crystalline structure of the dried powder samples was assessed by X-ray diffraction (XRD) with a Philips X'Pert diffractometer using $\text{Cu K}\alpha$ ($\lambda = 1.54 \text{ \AA}$) as incident radiation, operating at 40 kV and 30 mA. To estimate the average crystallite size, the Debye-Scherrer equation was employed using X-ray diffraction data of the samples. Transmission electron microscopy was carried out in a JEM-1011 microscope with the accelerating voltage of 100 kV. For the TEM study, a very small amount of the powder sample was first dispersed in isopropyl alcohol (IPA) by ultra-sonication. A drop of that solution was taken on a carbon grid for TEM imaging, which was purchased commercially. UV-vis absorption spectra were recorded using a Varian-Cary Bio UV-vis spectrophotometer by dispersing the samples in ethanol at room temperature.

2.3 Photo Reactor

Figure 1 shows the schematic diagram of the photo reactor used in this study. All the experiments are performed in a cylindrical photo reactor with a total volume of 1.0 L. The reactor is made of glass and covered with an aluminum sheet to prevent loss of UV light. The reactor is capped by a rubber membrane which has in its center a quartz tube for placing the UV lamp. It is provided with inlets for feeding oxygen gas flow, and port for withdrawing samples. A Teflon coated magnetic stirring bar was placed in the reactor bottom for homogenization. Methyl orange ($\text{C}_{14}\text{H}_{14}\text{N}_3\text{NaO}_3\text{S}$), a widely used dye, was employed as a representative dye pollutant to evaluate the photocatalytic activity of the three ZnO samples (60°C , 80°C and commercial ZnO). The experiments were performed in the reactor charged with 900 ml of aqueous solution containing 0.02 g.L^{-1} of methyl orange and 0.1 g.L^{-1} of ZnO powder. The suspensions were ultrasonically sonicated for 20 min and magnetically stirred in dark during the irradiation. The irradiation of the suspensions was carried out using an UV lamp (8 W), that emits ultraviolet light of 365 nm, fixed on the central axis of the reactor. The transmittance of the filtered methyl orange solution with a $0.2 \mu\text{m}$ membrane filter was measured using a UV-visible spectrophotometer (Q798U QUIMIS) at intervals of 30 min and the total irradiation time is 12 h.

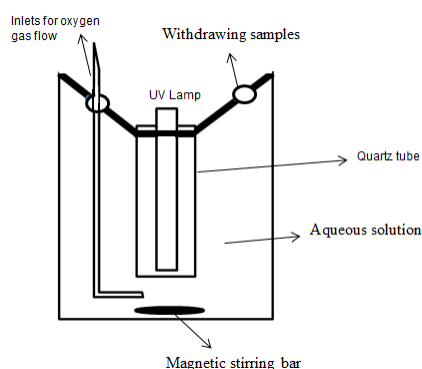


Figure 1: A schematic diagram of the photo reactor.

3. Results and discussion

The crystalline structure of the samples formed at 60 °C (ZnO 60) and 80 °C (ZnO 80) by chemical reaction between NaOH and ZnCl₂ were examined by X-ray diffraction (Figure 2). In the same figure, the diffraction pattern of commercial ZnO (ZnO *) is shown for comparison. All the diffraction peaks of the ZnO samples can be indexed to (1 0 0), (0 0 2), (1 0 1), (1 0 2), (1 1 0), (1 0 3), (2 0 0), (1 1 2) and (2 0 1) diffraction planes reported at the ICSD database (Card No. 57 450). The absence of extra peaks, which could be related to impurities, indicates that the ZnO samples produced in this study have high purity.

The average crystallite size of the ZnO samples was obtained by measuring the broadening of diffraction lines and using the Scherrer equation (Wang et al., 2008) of the (1 0 1) reflection:

$$D = k\lambda/\beta\cos\theta \quad (1)$$

where λ is the wavelength of Cu K α radiations ($\lambda = 1.54 \text{ \AA}$), $\beta = B - b$, θ is the Bragg's angle, and K is related to the crystallite shapes ($K = 0.91$). The average crystallite size of the ZnO samples were $\sim 28 \text{ nm}$ (ZnO 60) and $\sim 24 \text{ nm}$ (ZnO 80). The average crystallite size of the commercial ZnO estimated by the Debye–Scherrer equation was about 55 nm.

Transmission electron microscopy was used to examine the morphological characteristics of the products synthesized at 60 °C and 80 °C (Figure 3). The TEM image of the ZnO sample obtained at 60 °C (Figure 3(a)) shows the presence of nanorods with average length of $\sim 102 \text{ nm}$ and average diameter (which is equivalent to average crystallite size) of $\sim 30 \text{ nm}$. The morphology of the ZnO sample synthesized at 80 °C is rod-like (Figure 3(b)), but the particles are shorter than those found in 60 °C. These particles have an average diameter of about 25 nm and an average length of about 60 nm. The TEM images of both samples (ZnO 60, ZnO 80) show large agglomeration of the ZnO particles.

The results above reveal that the reaction temperature affects the nanorods size, and consequently the formation mechanism (nucleation and growth) of the ZnO particles. At the beginning of the reaction, the low precursor concentration in the presence of highly basic NaOH causes the immediate formation of Zn(OH)₂ clusters. These clusters become ZnO nuclei under supersaturation condition. The nucleation rate is strongly influenced by temperature and is faster at higher temperatures (Shevchenko et al., 2003). Thus, at 80 °C a large quantity of ZnO nuclei is generated, which reduces the number of clusters in the reaction medium. The reduction in the amount of reagents may disrupt the formation of new nuclei. Then, residual clusters that were not converted into ZnO nuclei are used for the growth of nanorods. The few growth units available in the reaction medium will limit the process of particle growth. Consequently, ZnO nanorods with a smaller final size than that of the 60 °C sample were obtained, as shown by TEM and XRD results.

Optical properties of the ZnO samples dispersed in absolute ethanol were investigated by UV–Visible spectroscopy at room temperature. A blank solution of ethanol was used as reference. The UV-Vis absorption spectra of the samples obtained at different reaction temperature are presented in Figure 4. The spectra in all cases behave similarly and the samples exhibit prominent exciton bands around 366 nm (60 °C) and 363 nm (80 °C). No other peak in the spectra confirms that the synthesized products are only ZnO (Wahab et al., 2011).

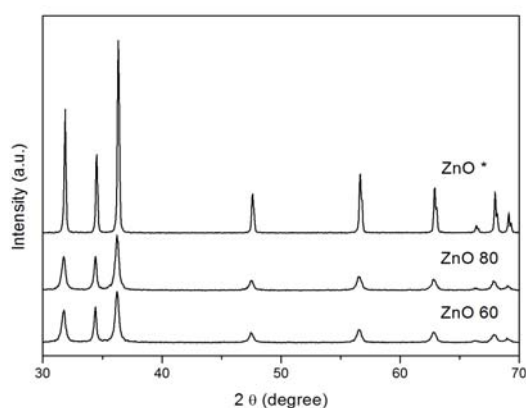


Figure 2: XRD of the ZnO samples obtained at different temperatures: (ZnO 60): 60 °C and (ZnO 80): 80 °C. XRD of the commercial ZnO (ZnO *) is also shown.

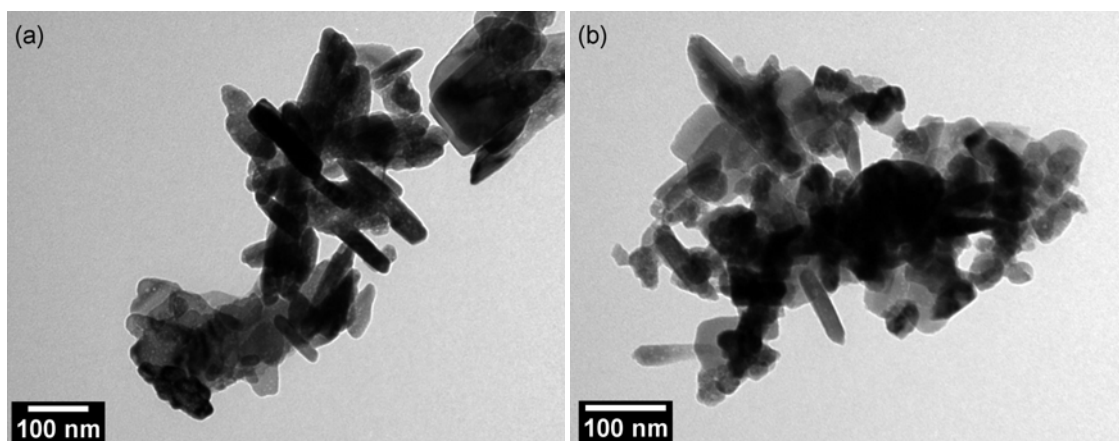


Figure 3: TEM images of the ZnO nanorods obtained at (a) 60 °C and (b) 80 °C via solochemical method.

Photocatalytic tests were carried out for all samples (ZnO 60, ZnO 80 and ZnO *). Methyl orange was used as a model organic compound. Figure 5 shows the effect of UV-light irradiation time on the photocatalytic discoloration of the methyl orange in the presence of ZnO powders. In the presence of commercial ZnO, 98 % of methyl orange was completely discoloured after 2 h of irradiation. However, only 20 % and 21 % of methyl orange were discoloured at 2 h of irradiation in the presence of ZnO 60 and ZnO 80, respectively. These results show that the photocatalytic discoloration of methyl orange using commercial ZnO is faster than using the ZnO nanorods obtained in this work. The poor efficiency of photocatalytic discoloration of the ZnO samples synthesized in this work is probably due to large agglomeration of particles as shown by TEM results.

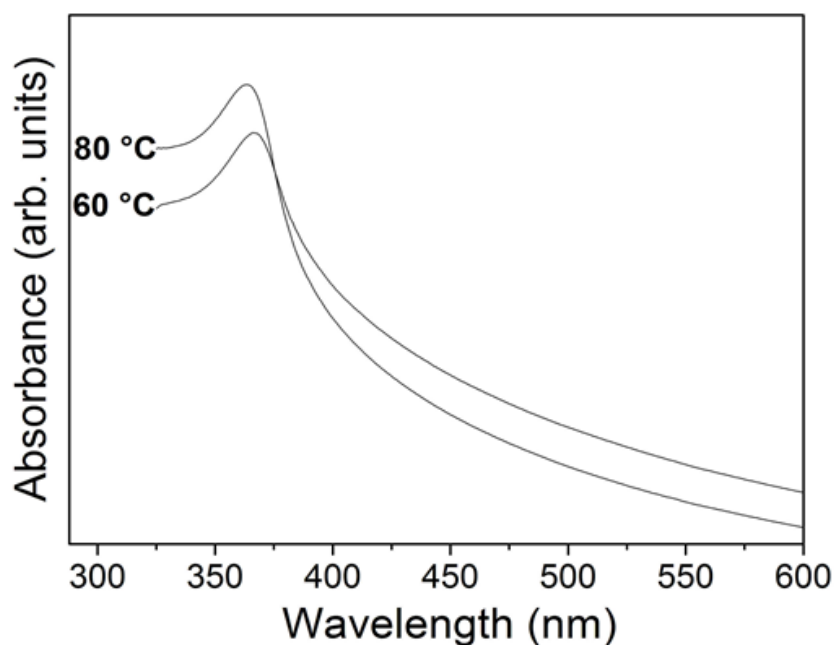


Figure 4: UV-Vis spectra of the ZnO nanostructures obtained at 60 °C and 80 °C in this work.

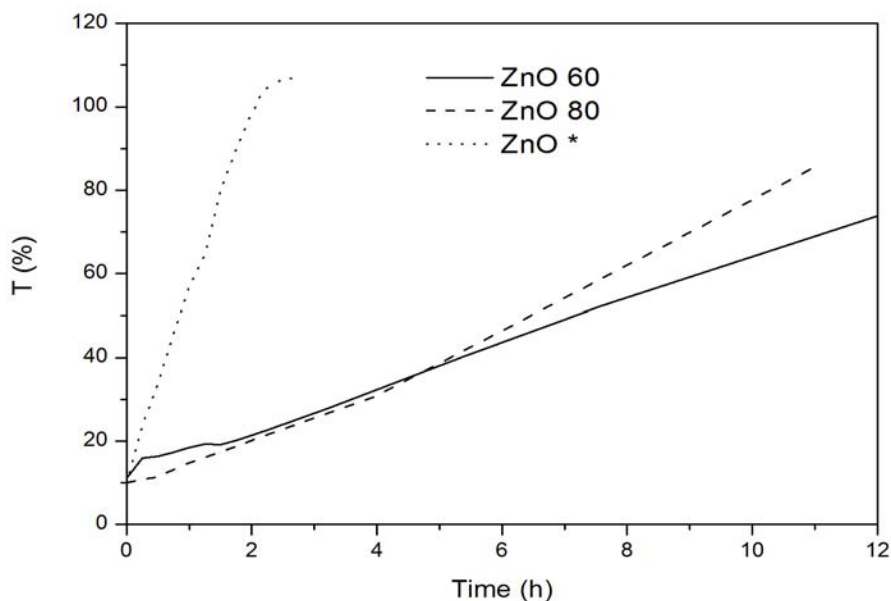


Figure 5; UV-light irradiation time on the photocatalytic discolouration of the methyl orange in the presence of ZnO powders: (ZnO 60): 60 °C and (ZnO 80): 80 °C obtained via solochemical technique; (ZnO*): commercial ZnO.

4. Conclusion

In this study, zinc oxide nanorods were successfully synthesized by solochemical method using zinc chloride and sodium hydroxide at relatively low refluxing temperature of 60 °C and 80 °C in a few hours. The present work outlines also some basic analyses of photocatalytic property of the products that was compared to commercial ZnO. The crystallinity of the synthesized zinc oxide nanorods were observed using X-ray diffraction and the morphology was analyzed by using TEM. In addition to these properties, photocatalytic activity was also studied in presence of methyl orange. The results clearly indicate that the synthesized ZnO nanorods have interesting photocatalytic activity for the discolouration of methyl orange dye with more than 10 h of irradiation.

5. Acknowledgements

Research supported by Central Laboratory of Electron Microscopy (LCME) of UFSC. The authors are grateful for the financial support of CAPES/PNPD.

References

- Caglar Y., Aksoy S., Ilican S., Caglar M., 2009, Crystalline structure and morphological properties of undoped and Sn doped ZnO thin films, *Supperlattices Microstruct.* 46, 469-475.
- Chakrabarti S., Chaudhuri B., Bhattacharjee S., Dasg P., Dutta B. K., 2008, Degradation mechanism and kinetic model for photocatalytic oxidation of PVC–ZnO composite film in presence of a sensitizing dye and UV radiation, *J. Hazard. Mater.* 154, 230-236.
- Chen Y., Yu R., Shi Q., Qin J., Zheng F., 2007, Hydrothermal synthesis of hexagonal ZnO clusters, *Mater. Lett.* 61, 4438-4441.
- Duffy G.M., Pillai S.C., McCormack D.E., 2007, A novel processing route for the production of nanoparticulate zinc oxide using an isophthalate precursor, *Smart Mater. Struct.* 16, 1379-1381.
- Gusatti M., Rosário J.A., Barroso G.S., Campos C.E.M., Riella H.G., Kuhn N.C., 2009, Synthesis of ZnO nanostructures in low reaction temperature, *Chemical Engineering Transactions*, 17, 1017-1021
- Gusatti M., Rosário J.A., Campos C.E.M., Kuhn N.C., Carvalho E.U., Riella H.G., Bernardin A.M., 2010, Production and characterization of ZnO nanocrystals obtained by solochemical processing at different temperatures, *J. Nanosci. Nanotechnol.* 10, 4348-4351.

- Gusatti M., Campos C.E.M., Rosário J.A., Souza D.A.R., Kuhnen N.C., Riella H.G., 2011, The rapid preparation of ZnO nanorods via low-temperatures solochemical method, *J. Nanosci. Nanotechnol.* 11, 5187-5192.
- Gusatti M., Campos C.E.M., Souza D.A.R., Kuhnen N.C., Riella H.G., Pizani P.S., 2012, Effects of reaction temperature on structural properties of ZnO nanocrystals prepared via solochemical technique, *J. Nanosci. Nanotechnol.* 12, 7986-7992.
- Haase M., Weller H., Henglein A., 1988, Photochemistry and radiation chemistry of colloidal semiconductors. Electron storage on zinc oxide particles and size quantization, *J. Phys. Chem.* 92, 482-487.
- Hu Y., Chen H.J., 2008, Preparation and characterisation of nanocrystalline ZnO particles from a hydrothermal process, *J. Nanopart. Res.* 10, 401-407.
- Huang M.H., Mao S., Feick H., Yan H., Yiyang W., Kind H., Weber E., Russo R., Yang P., 2001, Room-temperature ultraviolet nanowire nanolasers, *Science*, 292, 1897-1899.
- Johnson J.C., Yan H., Schaller R.D., Haber L.H., Saykally R.J., Yang P., 2001, Single nanowire lasers, *J. Phys. Chem.* B105, 11387-11390.
- Kajbafvala A., Ghorbani H., Paravar A., Samberg J.P., Kajbafvala E., Sadrnezhad S.K., 2012, Effects of morphology on photocatalytic performance of zinc oxide nanostructures synthesized by rapid microwave irradiation methods, *Superlattices and Microstruct.* 51, 512-522.
- Kanade K.G., Kale B.B., Aiyer R.C., Das B.K., 2006, Effect of solvents on the synthesis of nano-size zinc oxide and its properties, *Mater. Res. Bull.* 41, 590-600.
- Kenanakis G., Katsarakis N., 2010, Light-induced photocatalytic degradation of stearic acid by c-axis oriented ZnO nanowires, *Appl. Cata. A: Gene.* 378, 227-233.
- Liu Y., Zhou J., Larbot A., Persin M., 2007, Preparation and characterization of nano-zinc oxide, *J. Mater. Process. Tech.* 189, 379-383.
- Lu X.H., Wang D., Li G.R., Su C.Y., Kuang D.B., Tong Y.X., 2009, Controllable electrochemical synthesis of hierarchical ZnO nanostructures on FTO glass, *J. Phys. Chem. C* 113, 13574-13582.
- Major C., Nemeth A., Radnóczy G., Czigan Z., Fried M., Labadi Z., Barsony I., 2009, Optical and electrical characterization of aluminium doped ZnO layers, *Appl. Surf. Sci.* 255, 8907-8912.
- Parida K.M., Dash S.S., Das D.P., 2006, Physico-chemical characterization and photocatalytic activity of zinc oxide prepared by various methods, *J. Colloid Interface Sci.* 298, 787-793.
- Shevchenko E.V., Talapin D.V., Schnablegger H., Kornowski A., Festin Ö., Svedlindh P., Haase M., Weller H., 2003, Study of nucleation and growth in the organometallic synthesis of magnetic alloy nanocrystals: the role of nucleation rate in size control of CoPt₃ nanocrystals, *J. Am. Chem. Soc.*, 125, 9090-9101.
- Rataboul F., Nayral C., Casanove M.J., Maisonnat A., Chaudret B., 2002, Synthesis and characterization of monodisperse zinc and zinc oxide nanoparticles from the organometallic precursor [Zn(C₆H₁₁)₂], *J. Organomet. Chem.* 643-644, 307-312.
- Siah F., Yang Z., Tang Z.K., Wong G.K.L., Kawasaki M., Ohtomo A., Koinuma H., Segawa Y., 2000, In-plane anisotropic strain of ZnO closely packed microcrystallites grown on tilted (0001) sapphire, *J. Appl. Phys.* 88, 2480-2483.
- Viswanatha R., Sapra S., Satpati B., Satyam P. V., Dev B. N., Sarma D. D., 2004, Understanding the quantum size effects in ZnO nanocrystals, *J. Mater. Chem.*, 14, 661-668.
- Wahab, R., Hwangl.H., KimY.S., Shin H.S., 2011, Photocatalytic activity of zinc oxide micro-flowers synthesized via solution Method, *Chemical Engineering Journal* 168, 359-366.
- Wang C., Xu B.Q., Wang X., Zhao J., 2005, Preparation and photocatalytic activity of ZnO/TiO₂/SnO₂ mixture, *J. Sol. St. Chem.* 178, 3500-3506.
- Wang Z., Zhang H., Zhang L., Yuan J., Yan S., Wang C., 2003, Low-temperature synthesis of ZnO nanoparticles by solid-state pyrolytic reaction, *Nanotechnology*, 14, 11-15.